

# PARAMETRIC B-SPLINE SNAKES ON DISTANCE MAPS—APPLICATION TO SEGMENTATION OF HISTOLOGY IMAGES

*S. Chandra Sekhar, François Aguet, Sébastien Romain, Philippe Thévenaz, and Michael Unser*

Biomedical Imaging Group,  
École Polytechnique Fédérale de Lausanne (EPFL),  
Switzerland.

Emails: {chandrasedkhar.seelamantula,francois.aguet,sebastien.romain,philippe.thevenaz,michael.unser}@epfl.ch

## ABSTRACT

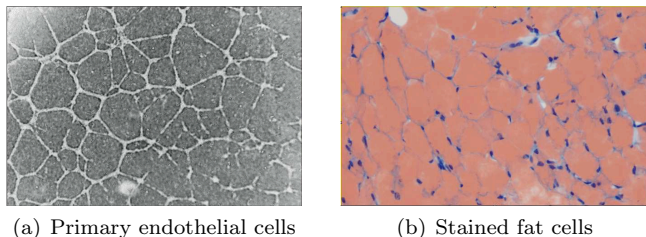
We construct parametric active contours (snakes) for outlining cells in histology images. These snakes are defined in terms of cubic B-spline basis functions. We use a steerable ridge detector for obtaining a reliable map of the cell boundaries. Using the contour information thus obtained, we compute a distance map and specify it as one of the snake energies. To ensure smooth contours, we also introduce a regularization term that favors smooth contours. A convex combination of the two cost functions results in smooth contours that lock onto edges efficiently and consistently. Experimental results on real histology images show that the snake algorithm is robust to imperfections in the images such as broken edges.

## 1. INTRODUCTION

Active contour models, also known as snakes, have proven to be effective tools for segmenting objects of interest in a given image. With a growing number of technological advances in medical and bioimaging modalities, the problem of segmentation has become more important than ever. Physicians and biologists are highly interested in semi-automated software that helps them outline specific organs or cells in medical/biological images. Computer-assisted segmentation tools reduce the inter and intra-human variability and can process huge stacks of images in a semi-automatic fashion with a minimal manual effort.

There exists a large variety of snake algorithms—point-based snakes [1], geometric snakes [2, 3], and parametric snakes [4, 5, 6, 7]. In this paper, we promote the use of parametric snakes where the bases are compactly-supported spline functions [8]. This choice offers some advantages such as computational simplicity, sparse representation, and flexibility in adapting to different snake energies. The spline framework also allows one to incorporate suitable smoothness criteria, which is somewhat difficult to ensure in a general curve-evolution approach. We use cubic B-splines because they have been shown to be efficient, not only from the point of view of parameterization, but also for optimization [7].

In this paper, we address the specific task of outlining cell images in histology measurements. Histology is a kind of microscopic anatomy in which thin slices of tissues are studied. The slices are obtained by using a mechanical instrument called a *microtome*. The typical tissue thickness varies from 2 to 25  $\mu\text{m}$ . Histology is an



(a) Primary endothelial cells

(b) Stained fat cells

Figure 1: Some examples of images used in histology studies.

essential tool of biological studies, in particular for disease diagnosis. In some cases, a staining agent is used to increase the contrast of the tissue being examined, and to see differences in cell morphology. For example, agents such as Hematoxylin impart blue color to the nuclei and pink to the cytoplasm. Figure 1 shows some examples—(a) is an image of primary endothelial cells and (b) that of stained fat cells. The image in Fig.1(a) is shown in grayscale; the primary objective is to outline the cells. Cell-outlining enables the computation of parameters of interest such as the cell size and area, as well as velocity when a sequence of time-lapse images is available. This aids in understanding cell growth when monitored over a period of time. For the results reported in this paper, we used endothelial cell images.

## 2. PARAMETRIC REPRESENTATION OF A CLOSED SNAKE USING B-SPLINES

A curve in the  $x-y$  plane can be described in a parametric fashion as  $\mathbf{r}(t) = (x(t), y(t))$ , where  $t$  is an arbitrary parameter. The one-dimensional parametric functions  $x(t)$  and  $y(t)$  can be described efficiently as a linear combination of suitable bases. We choose bases derived from a scaling function  $\beta(t)$  and employ a representation that has a shift-invariant flavor; i.e., an expansion of the type

$$x(t) = \sum_{k=-\infty}^{\infty} c_{xk} \beta(t-k), \text{ and} \quad (1)$$

$$y(t) = \sum_{k=-\infty}^{\infty} c_{yk} \beta(t-k), \quad (2)$$

where the coefficients  $\{(c_{xk}, c_{yk}), k \in \mathbb{Z}\}$  are the weights attached to the scaling function and its integer translates. In the spline literature, the coefficients are called

knot points.

The commonly-used active contours are typically closed curves specified by a finite number of knot points  $M$ . Therefore, the bases are periodized and this reduces the infinite summation in (1) and (2) to a finite one, as given below.

$$x(t) = \sum_{k=0}^{M-1} c_{xk} \beta_P(t-k), \text{ and} \quad (3)$$

$$y(t) = \sum_{k=0}^{M-1} c_{yk} \beta_P(t-k), \quad (4)$$

where

$$\beta_P(t-k) = \sum_{k=-\infty}^{\infty} \beta(t-kM) \quad (5)$$

is the  $M$ -periodized basis function.

We choose  $\beta(t)$  to be the cubic B-spline, which has a piecewise-polynomial definition:

$$\beta(x) = \begin{cases} \frac{2}{3} - |x|^2 + \frac{|x|^3}{2}, & 0 \leq |x| < 1 \\ \frac{(2-|x|)^3}{6}, & 1 \leq |x| < 2 \\ 0, & 2 \leq |x|. \end{cases} \quad (6)$$

The cubic B-spline is an optimal interpolating function and satisfies the minimum-curvature property [6].

### 3. SNAKE FORMULATION

An active contour is a curve described by an ordered set of points, and it evolves starting from a user-specified position (the initialization) to some boundary within the image. The process of evolution is formulated as an optimization problem, and the associated cost function is called the *snake energy*. Broadly, snake energies comprise the image energy  $E_{image}(\Theta)$ , which guides the snake towards the boundary of interest; and the internal energy of the curve  $E_{curve}(\Theta)$  to ensure smooth contours. The parameter vector  $\Theta$  is a collection of the coefficients  $\{(c_{xk}, c_{yk}), 0 \leq k \leq M-1\}$ . The optimal snake is thus specified by a parameter  $\Theta^*$ , which is defined as

$$\Theta^* = \arg \min_{\Theta} (E_{image}(\Theta) + E_{curve}(\Theta)). \quad (7)$$

The choice of the snake energies is crucial as it directly determines the quality of image segmentation. It is widely accepted that any one set of energies is, in general, not suitable for all kinds of images. Appropriate energies have to be defined depending on the type of images and the application.

### 4. SNAKE ENERGIES

#### 4.1 Steerable filters for ridge detection

The key to an efficient segmentation algorithm is to extract good edge information, irrespective of the orientation of the edges, such as the ones in Fig. 1(a). A ridge detection algorithm based on steerable filters is the perfect choice for this purpose. In the following, we describe the details of the steerable filters that we used

in our implementation.

Given an image function  $f(\mathbf{x})$  and a template  $h(\mathbf{x})$ , the problem of detecting edges is formulated as

$$\theta^*(\mathbf{x}) = \arg \max_{\theta} (f(\mathbf{x}) * h(\mathbf{R}_{\theta} \mathbf{x})), \quad (8)$$

$$r^*(\mathbf{x}) = f(\mathbf{x}) * h(\mathbf{R}_{\theta^*} \mathbf{x}), \quad (9)$$

where  $\theta^*$  and  $r^*$  are the orientation and magnitude of the edge, respectively; and  $\mathbf{R}_{\theta}$  is the unitary rotation matrix:

$$\mathbf{R}_{\theta} = \begin{pmatrix} \cos \theta & \sin \theta \\ -\sin \theta & \cos \theta \end{pmatrix}. \quad (10)$$

Direct implementation of the optimization in (8) is computationally expensive. It requires an iterative solution that involves the convolution of the orientated template with the image for every intermediary angle  $\theta$ , or alternatively, relies on sampling over  $\theta$ .

The class of steerable filters first introduced by Freeman et al. [9] allows to solve the detection problem efficiently. The rotated version of the filters, consisting of partial derivatives of a Gaussian, is obtained by taking a linear combination of a small number of base templates, which are themselves partial derivatives of a Gaussian. Jacob et al. [10] extended the concept and introduced a framework for the design of templates that optimally match a given type of feature (i.e., an idealized edge or a ridge). The templates consist of a linear combination of partial derivatives of a Gaussian  $g(x, y)$ :

$$h(x, y) = \sum_{k=1}^M \sum_{i=0}^k \alpha_{k,i} \frac{\partial^{k-i}}{\partial x^{k-i}} \frac{\partial^i}{\partial y^i} g(x, y), \quad (11)$$

where, by linearity,  $h(x, y)$  is steerable, and where the weights  $\alpha_{k,i}$  are optimized to maximize the signal-to-noise ratio, localization, and regularity of the template, and where  $M$  is the order of the template.

The convolution with the template oriented at an arbitrary angle is expressed as

$$f(\mathbf{x}) * h(\mathbf{R}_{\theta} \mathbf{x}) = \sum_{k=1}^M \sum_{i=0}^k b_{k,i}(\theta) f_{k,i}(\mathbf{x}), \quad (12)$$

$$f_{k,i}(x, y) = f(x, y) * \left( \frac{\partial^{k-i}}{\partial x^{k-i}} \frac{\partial^i}{\partial y^i} g(x, y) \right), \quad (13)$$

where the coefficients  $b_{k,i}(\theta)$  are polynomials in  $\sin \theta$  and  $\cos \theta$ . The optimal orientation is obtained by solving

$$\sum_{k=1}^M \sum_{i=0}^k \frac{\partial}{\partial \theta} b_{k,i}(\theta) f_{k,i}(\mathbf{x}) = 0 \quad (14)$$

for  $\theta$ ; for orders up to  $M = 4$ , this is achieved analytically. In this work, we use the fourth-order ridge detector derived from the optimization in [10]. The only free parameter in this family of detectors is the standard deviation  $\sigma$  of the Gaussian upon which it is based. In practice,  $\sigma$  needs to be chosen to match the template width to the relevant feature width. Figure 2 shows the results of applying the steerable detector to a sample histology image. Note that the steerable filter results in a good detection of the cell walls, and a significant increase in contrast.

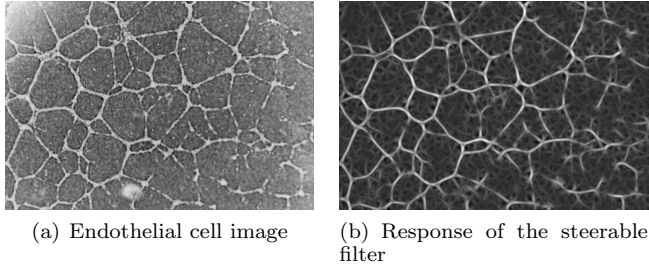


Figure 2: Cell boundary enhancement using the steerable filter.

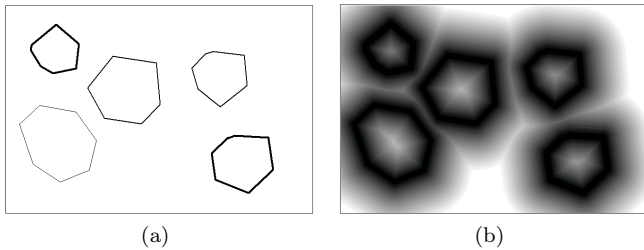


Figure 3: (a) Synthesized edge map and (b) the associated distance map.

## 4.2 Distance map

The next step is to use the edge information in defining an energy function that guides the snake to the cell boundaries. Typically, histology images contain a large collection of connected cells, where the inter-cell boundaries appear as facets. The problem of snake optimization is equivalent to moving the nodes of the snake to the nearest facet. This information is best captured in the form of a distance map. A distance map is a two-dimensional function which assigns to each pixel a value which is the distance from the pixel to the nearest edge. However, before we can do this, we must suppress the spurious noisy edges in the steerable filter response as much as possible. One way to accomplish this objective is to use a thresholding function. We use the Lloyd-Max quantization algorithm to determine the optimal threshold value. The result of thresholding is a two-level image which largely retains the genuine edges, and suppresses the spurious ones.

To compute the distance map, several algorithms are available, and we use the simplest of them. Our computation is based on a finite length two-dimensional mask whose entries are the Euclidean distances from the pixel position to the center of the mask. A synthesized edge map and the associated distance map are shown in Fig. 3. The distance map itself is used as the image energy in the snake optimization.

Loosely speaking, the distance map is like a mountain range, with the peak of a mountain lying in the inside of a cell; the foot of the mountain is likened to the boundary between adjacent cells. If a snake is initialized on the top of a mountain, by sheer gravity, it should go to the foot of the mountain. This philosophy will work perfectly when the images are noise-free and when the edge information is intact. However, arti-

facts in the images such as blobs or spurious edges that remain even after thresholding create spurious local optima in the distance map. In the snake optimization process, these local optima attract the nearest nodes, as a result of which, the snakes tend to have sharp corners. In some cases, the snake gets stuck in a local optimum and further curve evolution ceases. To push the nodes out of such spurious optima, and to ensure smooth contours, we add a regularizing function, which is described next.

## 4.3 Regularization

The regularizing function is based on the curvilinear energy [7], and is given by

$$E_{curv} = \int_0^M \left| |\mathbf{r}'(t)|^2 - c \right|^2 dt, \quad (15)$$

where

$$c = \frac{1}{M^2} \left( \int_0^M (x'(t)^2 + y'(t)^2)^{\frac{1}{2}} dt \right)^2, \quad (16)$$

and where

$$|\mathbf{r}'(t)|^2 = x'(t)^2 + y'(t)^2. \quad (17)$$

When the active contour evolves under the influence of  $E_{curv}$ , the knots are moved tangential to the curve, thus bringing it to the curvilinear abscissa. This particular energy term also goes well with the choice of the B-spline scaling function because it yields a minimum curvature provided that the parameterization is in the curvilinear abscissa.

## 4.4 Snake optimization

The total snake energy is a convex combination of the distance map function and  $E_{curv}$ . The weights attached to the energies are flexible and determine the tradeoff between the adhesion to cell boundaries, and smooth evolution. To optimize the snake coefficients, we use an iterative Powell-type algorithm. The partial derivatives of the energies with respect to the spline coefficients are computed in the same fashion as proposed in [7].

## 5. EXPERIMENTAL RESULTS

The optimization software is implemented as a Java plugin for ImageJ [11]. The weights attached to the energies can be controlled by means of a sliding bar. The plugin always loads an initial contour, which can be resized, moved or freely rotated by the user. Since snakes are known to be attracted to local optima, it is important to ensure that the initialization is not too far from the cell boundary of interest.

An example of snake optimization is shown in Fig. 4. Although the edges are broken, the regularization term ensures that the contours are smooth. Figure 5 shows an initialization which is away from the cell boundary. Even in this case, the snake nodes are driven outwards, smoothly, to the nearest edges. In this particular example, the edge information is not quite reliable and the snake converges to the best possible solution (Fig. 5(c)). Our graphical interface enables the user to interact with

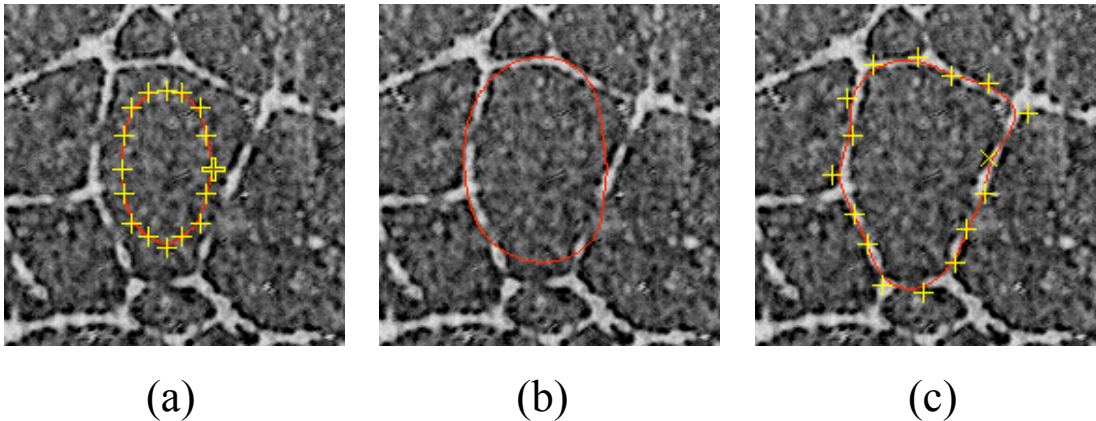


Figure 4: (Color online) Robustness of the snake algorithm to broken edges: (a) manual initialization, (b) evolving contour, and (c) converged snake.

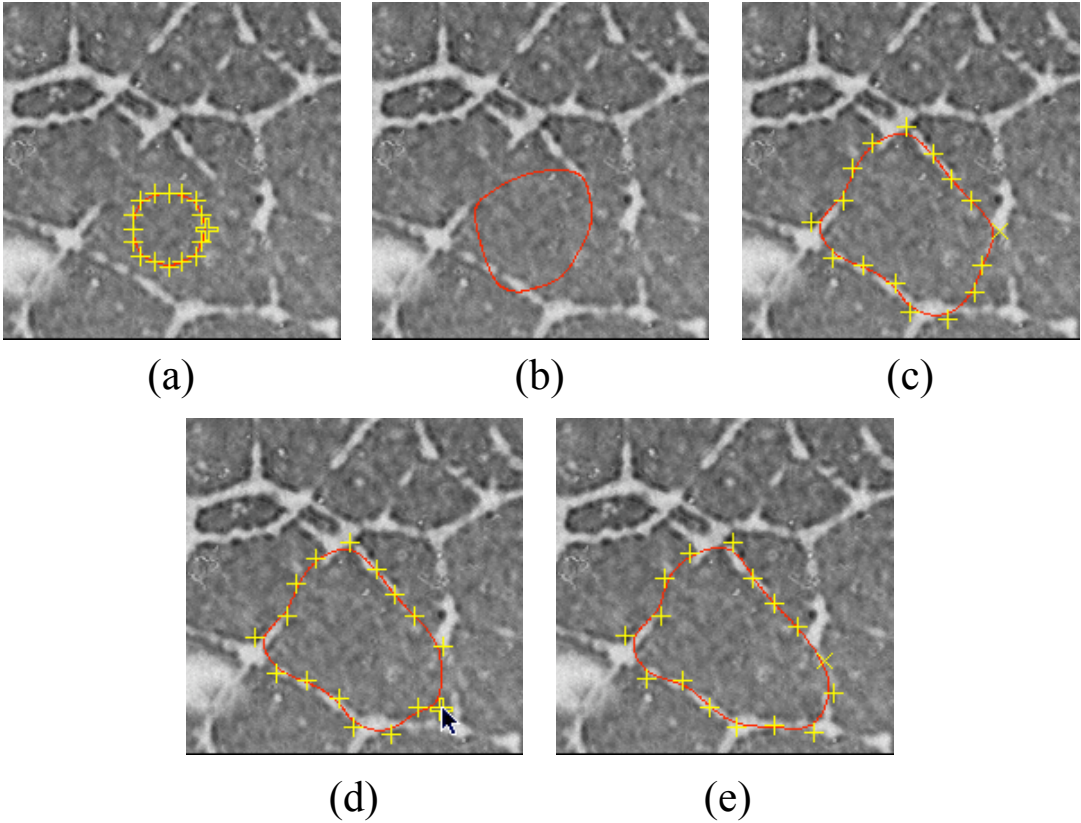


Figure 5: (Color online) Interactability of the snake software: (a) manual initialization, (b) evolving contour, (c) snake after intermediary convergence, (d) manual readjustment of a knot point, and (e) converged snake.

the active contour. Figure 5(d) shows, for example, how a user could easily readjust one of the nodes and set the optimizer running again. The converged snake is shown in Fig. 5(e).

## 6. CONCLUSION

In this paper, we have addressed active-contour-based cell-outlining with applications to histology. Keeping in view the geometric and intensity structure of the images, we have defined one of the snake energies as the distance map function. A novelty of our approach is that we apply a steerable ridge detector to obtain the edge information and use it to compute the distance map. We have also included a regularization term that drives the contour to the edges in a smooth fashion. Experimental results show that the new snake algorithm is robust to broken edges and other artifacts in the image. Our software also allows for interaction with the active contour, making it a useful and reliable semi-automatic tool for the biologists.

## Acknowledgments

The authors would like to thank Carol Murphy, Biomedical Research Institute, Foundation for Research and Technology-Hellas, University of Ioannina, Greece for providing us with the images that we used in this paper.

This work was supported in part by the Center for Biomedical Imaging (CIBM) of the Geneva-Lausanne Universities and the EPFL.

## REFERENCES

- [1] M. Kass, A. Witkin, and D. Terzopoulos, "Snakes: Active contour models," *Int. J. Comput. Vis.*, vol. 1, pp. 321–332, 1988.
- [2] V. Casselles, R. Kimmel, and G. Sapiro, "Geodesic active contours," in *Proc. Int. Conf. Computer Vision*, 1995.
- [3] R. Malladi, J. A. Sethian, and B. C. Vemuri, "Shape modeling with front propagation: A level-set approach," *IEEE Transactions on Pattern Analysis and Machine Intelligence*, vol. 17, pp. 158–174, 1995.
- [4] S. Menet, P. Saint-Mark, and G. Medioni, "B-snakes: Implementation and application to stereo," in *Proc. Image Understanding Workshop*, 1990, pp. 720–726.
- [5] M. A. Figueiredo and J. M. N. Leitao, "Unsupervised contour representation and estimation using b-splines and a minimum description length criterion," *IEEE Transactions on Image Processing*, vol. 9, pp. 1075–1087, June 2000.
- [6] P. Brigger, J. Hoeg, and M. Unser, "B-Spline snakes: A flexible tool for parametric contour detection," *IEEE Transactions on Image Processing*, vol. 9, no. 9, pp. 1484–1496, September 2000.
- [7] M. Jacob, T. Blu, and M. Unser, "Efficient energies and algorithms for parametric snakes," *IEEE Transactions on Image Processing*, vol. 13, no. 9, pp. 1231–1244, September 2004.
- [8] M. Unser, "Splines: A perfect fit for signal and image processing," *IEEE Signal Processing Magazine*, vol. 16, no. 6, pp. 22–38, November 1999, IEEE Signal Processing Society's 2000 magazine award.
- [9] W.T. Freeman and E.H. Adelson, "The design and use of steerable filters," *IEEE Transactions on Pattern Analysis and Machine Intelligence*, vol. 13, no. 9, pp. 891–906, 1991.
- [10] M. Jacob and M. Unser, "Design of steerable filters for feature detection using Canny-like criteria," *IEEE Transactions on Pattern Analysis and Machine Intelligence*, vol. 26, no. 8, pp. 1007–1019, 2004.
- [11] W. Rasband, "ImageJ," *U. S. National Institutes of Health, Bethesda, Maryland, USA*, <http://rsb.info.nih.gov/ij/>. 1997–2008.